

The Mesohellenic Trough and the Paleogene Thrace Basin on the Rhodope Massif, their Structural Evolution and Geotectonic Significance in the Hellenides

Kilias AD^{1*}, Vamvaka A¹, Falalakis G¹, Sfeikos A¹, Papadimitriou E², Gkaraouni CH² and Karakostas B²

¹Department of Geology, Aristotle University of Thessaloniki, Greece

²Department of Geophysics, Aristotle University of Thessaloniki, Greece

Abstract

Based on structural analysis and lithostratigraphic data, as well as geological mapping, the Paleogene part of the Thrace Basin (THB) in NE Greece (including the Paleogene deposits of the Axios Basin, AXB) was compared with the Mesohellenic Trough (MHT) in NW Greece. Both basins are characterized by a thick sedimentary sequence of molassic-type strata (3-5 km thickness) of Tertiary age, overlain unconformably by Miocene-Pliocene and Quaternary deposits. Molassic sedimentation started almost simultaneously in both areas during the Mid-Late Eocene but it finished in different time, in the Mid-Late Miocene for the MHT and the Late Oligocene for the THB, respectively. Sedimentation in THB was also linked with an important calc-alkaline and locally shoshonitic, acid to andesitic magmatism of Eocene-Oligocene age. We interpreted the MHT as a polyhistory strike-slip and piggy-back basin, above the westward-emplacing Neotethyan ophiolites and Pelagonian units on the cold Hellenic accretionary prism. In contrast to the MHT, the studied portion of the THB evolved as a Paleogene supra-detachment basin above the strongly extended during the Eocene-Oligocene Rhodope metamorphic province. The syn-depositional magmatic products, linked possibly with subduction processes in Pindos or Axios ocean(s). In any case, MHT and THB are related to inferred oblique convergence of the Apulia plate and the internal Hellenic units.

Keywords: Basin analysis; Molasse; Hellenides; Extension; Compression; Transpression

Introduction

Sedimentary basins and their filling products give important information for the structural evolution of orogenic belts and have been broadly used as guide indicators for the analysis of tectonic events related to plate movements.

There are numerous different shapes of sedimentary basins. They can be approximately circular or elongate depressions, troughs, or embayments, but often they have irregular boundaries. Most of the recent attempts to classify sedimentary basins were based on the modern concepts of global plate tectonics, as well as regional tectonics. We distinguish basins related to extension, compression and strike-slip movements during plate convergence or divergence. Based on the modern concept of global plate tectonics, the different types of sedimentary basins can be grouped as following [1,2] I. Continental, intracratonic sag basins II. Continental fracture basins, including the rift basins and supradetachment basins III. Basins on passive continental margins IV. Oceanic sag basins V. Basins related to subduction or active continental margins and island arc systems, including the deep-sea trenches, forearc- and backarc basins, VI. Basins related to continental collision, including the foreland and retroarc basins, usually with substratum of continental origin and VII. Strike-slip and wrench basins, including the transtensional (pull-apart) or transpressional basins.

Crustal subsidence (tectonic, thermal or sediment overload subsidence) is the main motor to initiate the basin formation and the sediment deposition but it is often associated, especially in an extensional tectonic regime, with uplift/exhumation of deep crustal metamorphic rocks, and formation of the metamorphic core complexes [3,4]. Two end-member of extensional basins can be rerecorded during a continuous extensional tectonism: rift basins and supradetachment basins. The differences in magnitude and rate of extension, volcanism, heat flow and structural architecture define the basin style and suggest the geotectonic setting related to the basin evolution [2-4].

The Mesohellenic Trough (MHT) in NW Greece [5-12] and the Thrace Basin (THB) in NE Greece [13-17], including its possible continuation into the Axios Basin (AXB) [18], constitute two large late to synorogenic Tertiary molassic-type basins in the Hellenides (Figure 1).

Younger, Neogene-Quaternary, unconformably overlying clastic sediments are not considered. Although these basins dominate with their size in the Hellenic orogen and the surrounding region (Figure 1) (Albania, Bulgaria, Turkey; References herein-see above), and while a lot of works with different approaches were published for each one basin, there still doesn't exist any comparison between the two basins until today, concerning their structural and stratigraphic evolution during the Alpine orogeny in the Hellenides, as well as their geodynamic setting. Besides, the knowledge of the structural evolution of both basins, as well as their geotectonic setting and structural relationships are of great importance to the better understanding of the tectonic evolutionary history of the Hellenides. Furthermore, it is known the great industrial potential of both basins due to gold-mineralizations and their possible hydrocarbon supplies [7,14,19].

This work is the first attempt to compare the evolutionary history of the two basins, as well as their paleogeographic and geotectonic setting in the Hellenic orogen, at least during their molassic-type sedimentation period, taking into account our previous studies on

*Corresponding author: Kilias AD, Department of Geology, Aristotle University of Thessaloniki, Greece, Tel: +30 231 099 6000; E-mail: kilias@geo.auth.gr

Received December 23, 2014; Accepted February 02, 2015; Published February 04, 2015

Citation: Kilias AD, Vamvaka A, Falalakis G, Sfeikos A, Papadimitriou E, et al. (2015) The Mesohellenic Trough and the Paleogene Thrace Basin on the Rhodope Massif, their Structural Evolution and Geotectonic Significance in the Hellenides. J Geol Geosci 4: 198. doi:10.4172/2329-6755.1000198

Copyright: © 2015 Kilias AD, et al. This is an open-access article distributed under the terms of the Creative Commons Attribution License, which permits unrestricted use, distribution, and reproduction in any medium, provided the original author and source are credited.

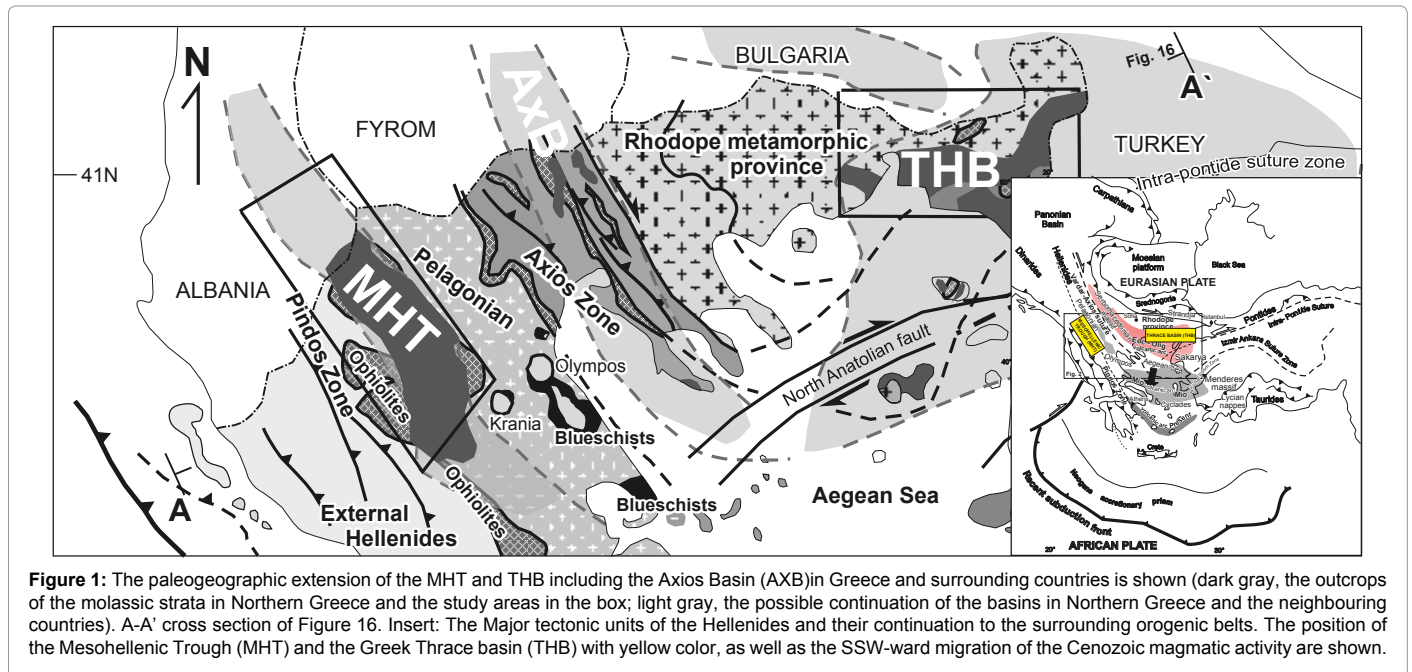


Figure 1: The paleogeographic extension of the MHT and THB including the Axios Basin (AXB) in Greece and surrounding countries is shown (dark gray, the outcrops of the molassic strata in Northern Greece and the study areas in the box; light gray, the possible continuation of the basins in Northern Greece and the neighbouring countries). A-A' cross section of Figure 16. Insert: The Major tectonic units of the Hellenides and their continuation to the surrounding orogenic belts. The position of the Mesohellenic Trough (MHT) and the Greek Thrace basin (THB) with yellow color, as well as the SSW-ward migration of the Cenozoic magmatic activity are shown.

both basins and any different published work referred to each basin's development. Furthermore, paleostress analysis based on fault-slip data, used in order to calculate the paleostress tensor, for each tectonic event affected the molassic strata of both basins. The direct stress inversion method of Angelier [20,21] was used. Although, both basins have a similar lithostratigraphic age, evolved mainly during the Tertiary, they differ in their structural evolution and geotectonic position in the frame of the Hellenic orogen and its evolutionary stages.

Geological Setting - Structural Evolution

The mesohellenic trough (MHT)

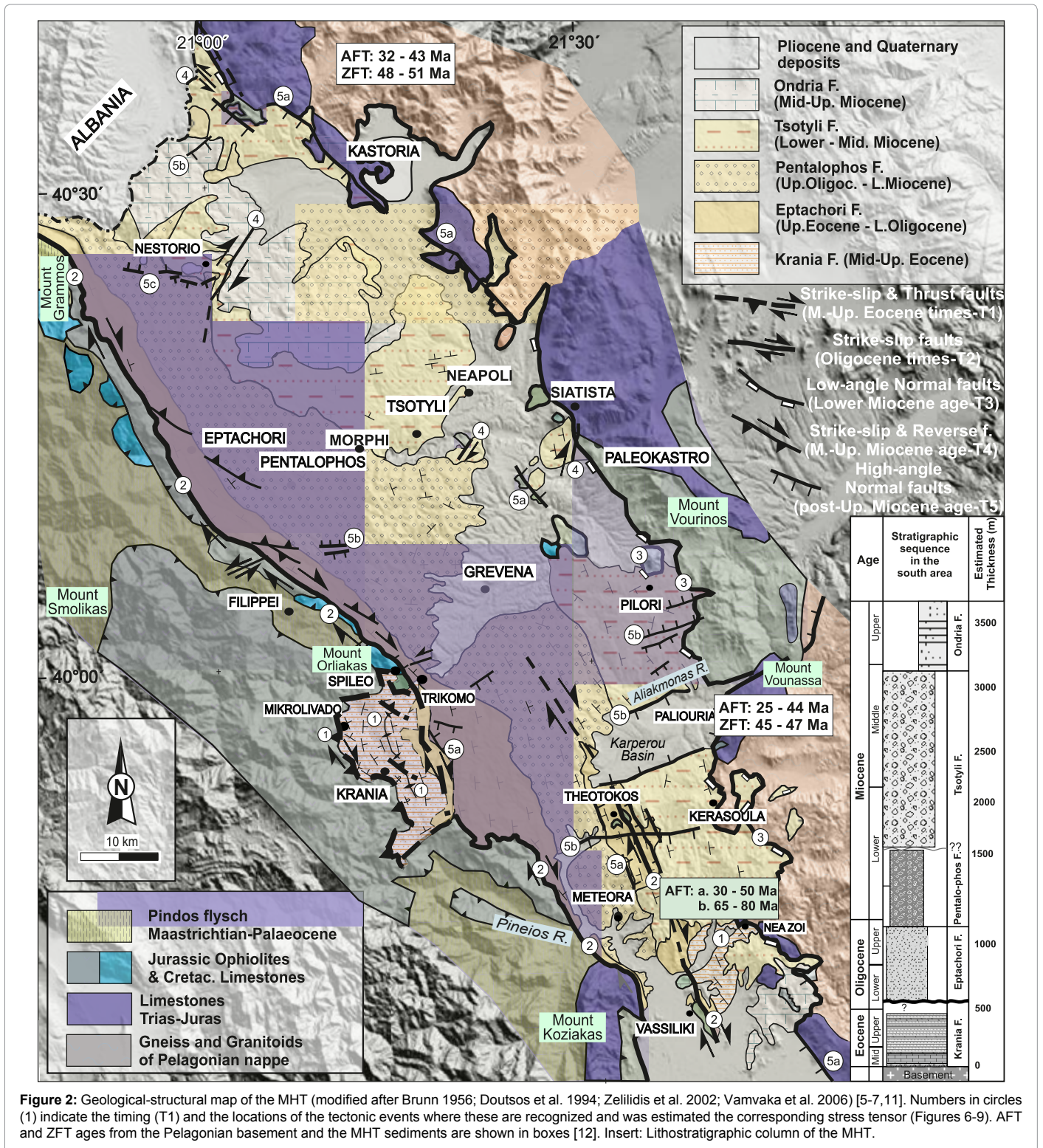
Lithostratigraphy: The Mesohellenic Trough (MHT) is located in north-western Greece and Albania, and has a length of more than 200 km and a width of 30-40 km (Figure 1). The basin developed from Mid-Late Eocene to Mid-Late Miocene time, related to the Alpine orogenic processes, and is sited parallel to the structural fabric of the Hellenides (i.e. NNW-SSE), between the Apulian plate (External Hellenides, non-metamorphic) and the Pelagonian nappe pile (Internal Hellenides, metamorphic).

The basin comprises five molassic-type formations (Figure 2) [5], overlying the Neo-Tethyan ophiolitic rocks and the transgressive Upper Cretaceous limestones or the western Pelagonian margin. Upper Miocene to Quaternary deposits overlie unconformably the molassic-type formations, which, from bottom to top, are (Figure 2) 1) Krania Formation of Middle-Upper Eocene age and a thickness of 1500 m [5,7,8,22]. 2) Eptachori Formation of Uppermost Eocene-Lower Oligocene age and a thickness of about 1000-1200 m [5,7]. 3) Pentalophos Formation of Upper Oligocene-Lower Miocene age, which attains a cumulative thickness of around 2500 m [5-8] while in the central part of the formation it is estimated to reach a maximum thickness of 4000 m [7]. 4) Tsotyli Formation of Lower-Middle Miocene age and a thickness of about 1500 m [5,7], and 5) Ondria Formation of Middle Miocene age (Burdigalian-Langhian), which remains only in a few places of the MHT with a thickness of about 350 m. With the exception of the Krania Formation in the westernmost

and the southeastern parts of the MHT, the other four formations were deposited parallel to one another from west to east, respectively (Figure 2), with an overall eastward migration of the depocenters and subsidence [5,23]. Accordingly, the Tsotyli formation directly rests on top of the Pelagonian continent along the eastern margin of the trough. At the western edge of the basin, the strata dip towards the ENE at steep angles; dips decrease progressively away from this basin margin, whereas along the eastern margin of the basin the strata dip with a low angle towards the WSW. As a result an asymmetrical syncline is formed in the Northern part of the basin, controlled by structural and depositional processes (Figure 2). In the south the MHT splits into two narrower synclines separated by an uplifted structure (Figures 2 and 3) (Theotokos-Vassiliki villages' areas) [6]. Furthermore, all formations, except the Eocene Krania Formation, become coarser towards the southern part characterized by extensive fan delta deposits [7].

Structural evolution: Numerous structural data, accrued from observations on geometry of kinematics, overprinted criteria, stratigraphic relationships and correlation between various structures, show that the basin experienced a complicated history with different tectonic episodes (T1-T5) (Figures 2-4) [11,12]. These events took place in semi-ductile to brittle conditions from Middle Eocene to Quaternary time. For the paleostress tensor calculation for each tectonic event the direct stress inversion method of Angelier [20,21] was considered. The solution is satisfyingly acceptable, if more than 80% of the fault-slip data from a site show a misfit angle less than 30° between the theoretical and real slip vector. The program My Fault-Version 1.03 [24] was used for the graphical presentation of the tectonic data.

The first stage (T1) of the basin's development, during the Middle-Late Eocene, was contemporaneous with the final emplacement of Pindos ophiolites on the External Hellenides and culminated in deformation and uplift of the Eocene strata. The Eocene sub-basins developed by crustal flexure and subsidence due to loading of the overthickened Hellenides accretionary prism. Basin evolution was associated with transpressional regime and dextral NNW-SSE trending strike-slip faults with a reverse, towards NE, dip-slip component.



Reverse faults and asymmetrical folds, with a main NE-ward vergence, are developed within the Eocene Krania deposits. During the ensuing followed basin closure and uplift at the end of Eocene, the sediments of the first sub-basins were deformed and placed with a high angle at the western basin margin, locally concordant with the adjacent ophiolitic rocks (Figures 2-4 and 5a). The paleostress analysis shows an almost

horizontal maximum principal σ_1 -stress axis NE-SW trending and an almost vertical minimum principal σ_3 - stress axis (Figures 4 and 6).

The second phase (T2) was dominated by strike-slip faults. Dextral strike-slip faults of NW-SE to NNW-SSE orientation controlled the subsidence and evolution of the basin from Early to Late Oligocene.

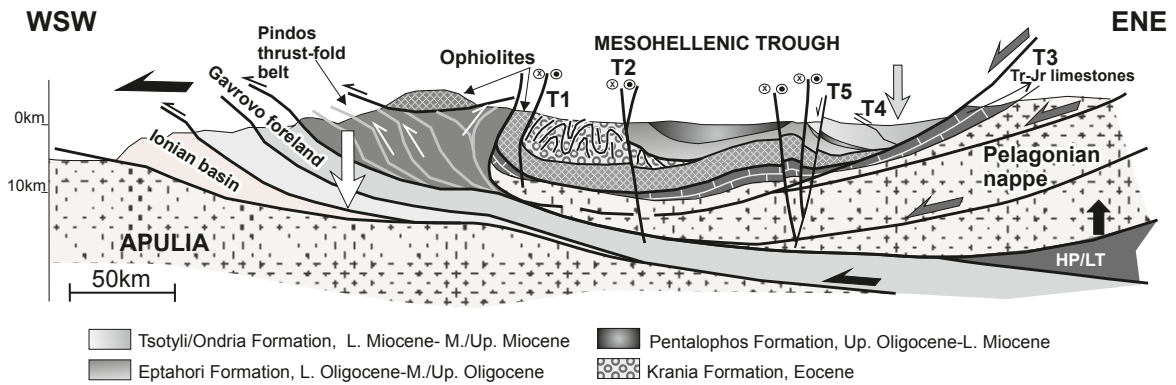


Figure 3: Schematic cross sections through the MHT showing the successive deformational stages related to the basinevolution [11].

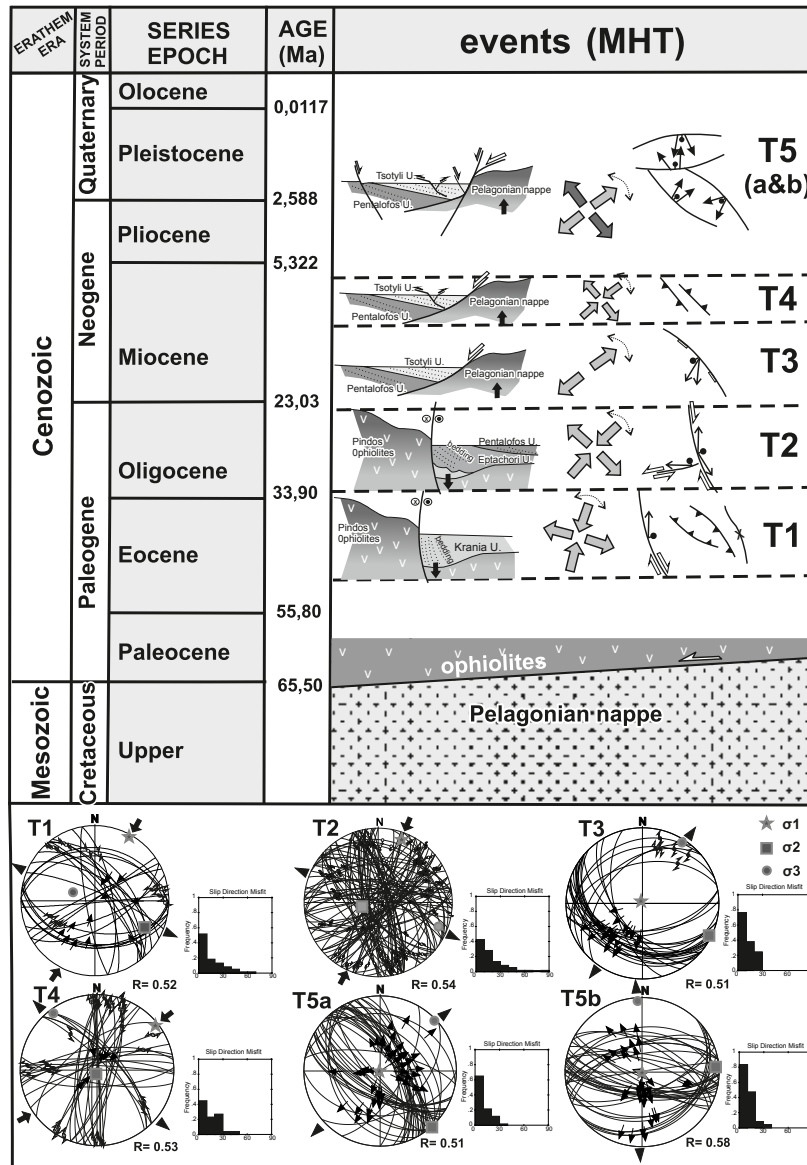


Figure 4: Distinctive features and kinematics of the main deformational events (T1 to T5) related to the MHT evolutionary history. Paleostress analysis diagrams ($\sigma_1 > \sigma_2 > \sigma_3$) for each tectonic event are shown (equal area, lower hemisphere). Fluctuation histograms of deviation angles (angle between the calculated slip vector and the measured slickenline) and stress ratio $R = \sigma_2 - \sigma_3 / \sigma_1 - \sigma_3$ are also indicated.

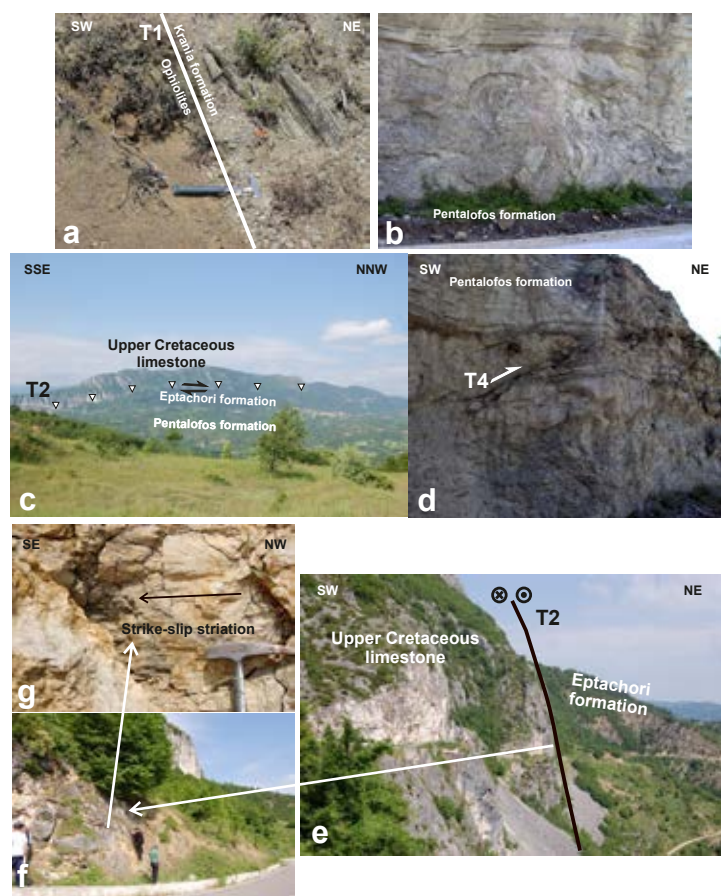


Figure 5: a. The tectonic contact (T1) between ophiolites and Kranea formation west of the Kranea village. b. Mass flows in the Pentalofos formation, road from Neapoli to Eptachori villages, near the Morphi village. c. Looking west, the marginal strike-slip fault (T2) between the Upper Cretaceous limestone of the Oriakas Mountain and the Eptachori formation, road Neapoli to Eptachori villages, near the Morphi village. d. Thrust fault (T4) in the Pentalofos formation, road Neapoli to Eptachori villages, near the Morphi village. e-g. The dextral strike-slip fault (T2) between the Upper Cretaceous limestone of the Oriakas mountain and the Eptachori Formation (e,g) with nearly horizontal striation on its fault plane (f), road to the Spilaion village on top of the Oriakas mountain.

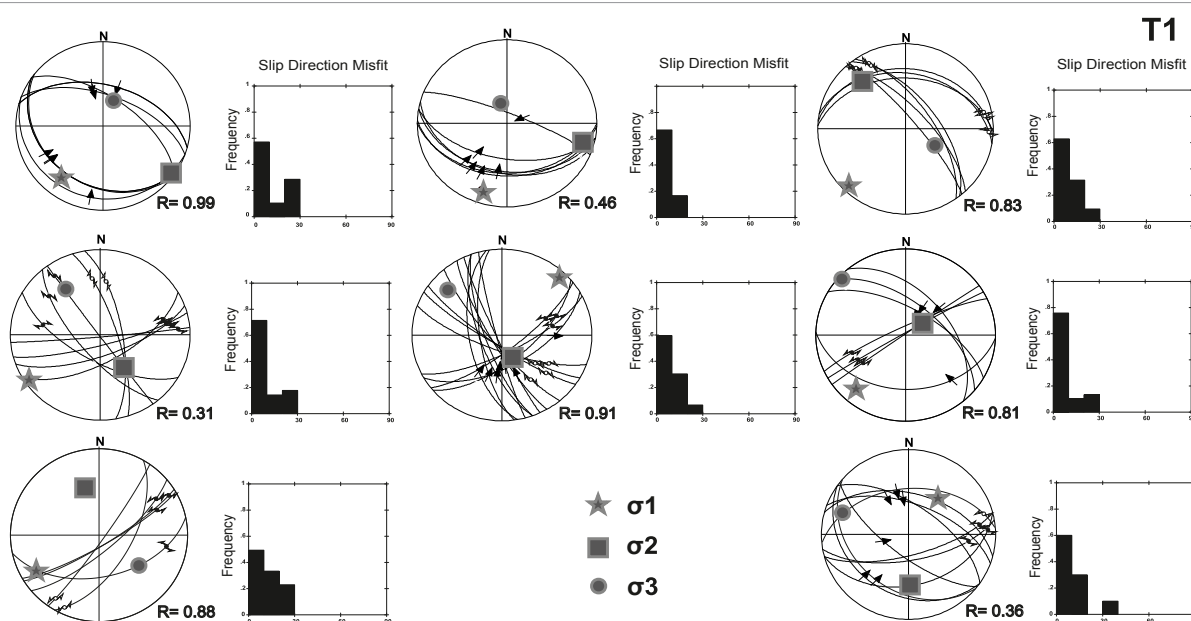


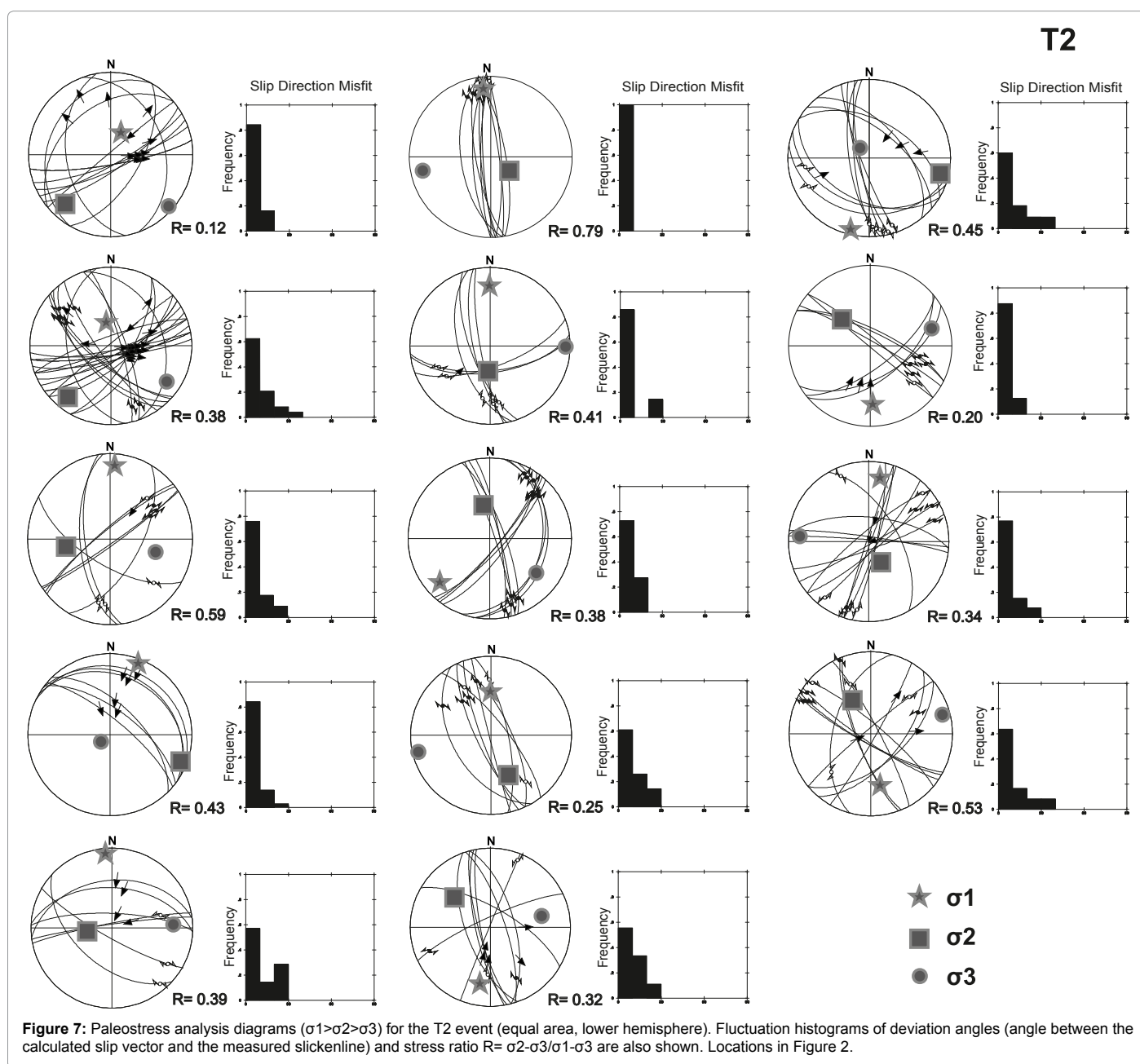
Figure 6: Paleostress analysis diagrams ($\sigma_1 > \sigma_2 > \sigma_3$) for the T1 event, affected only the Kranea Formation (equal area, lower hemisphere). Fluctuation histograms of deviation angles (angle between the calculated slip vector and the measured slickenline) and stress ratio $R = \sigma_2 - \sigma_3 / \sigma_1 - \sigma_3$ are also shown. Locations in Figure 2.

They define the western boundary of the MHT between basement rocks and the Eptachori Formation (Figures 2-4 and 5c-5g). Sinistral strike-slip fault zones along the western boundaries of the MHT are interpreted as riedl-structures. Strike-slip faults, positive flower structures and rare compressional structures (Figures 3 and 4) have been developed under a transpressional tectonic regime. It is characterized by a decrease in intensity towards the East and a small shift of the, low angle plunging, maximum principal stress axis (σ_1) from NE-SW to NNE-SSW, showing a small change in direction compared with the first T1 event. NW-SE to WNW-ESE trend shows respectively the minimum stress axis (σ_3) with a low also plunge, towards ESE or WNW (Figures 4 and 7).

The third phase (T3) was characterized by low-angle normal faulting along the eastern boundary of MHT during the Early-Middle Miocene,

causing the subsidence at that part of the trough (Figures 2-4). T3 was associated with the Oligocene-Miocene syn- to late orogenic collapse and detachment of the Pelagonian nappes [25-27]. The evolution of the sedimentary basin ended around Middle-Upper Miocene, followed later by rapid uplift and marine regression. The minimum σ_3 -stress axis was computed almost horizontal with a NE-SW orientation, whereas the maximum σ_1 -stress axis are nearly vertical, indicating the extensional stress regime during T3 event (Figures 4 and 8a).

A compressional event occurred during the Late Miocene times of relatively local importance, related to oblique reverse faults with a main, towards NE sense of movement, as well as strike-slip faults (T4) (Figures 2, 4 and 5d). T4 faults cut all the MHT molassic formations but not the younger postmolassic, Pliocene deposits of the basin. The paleostress analysis suggested that the stress regime during T4 event



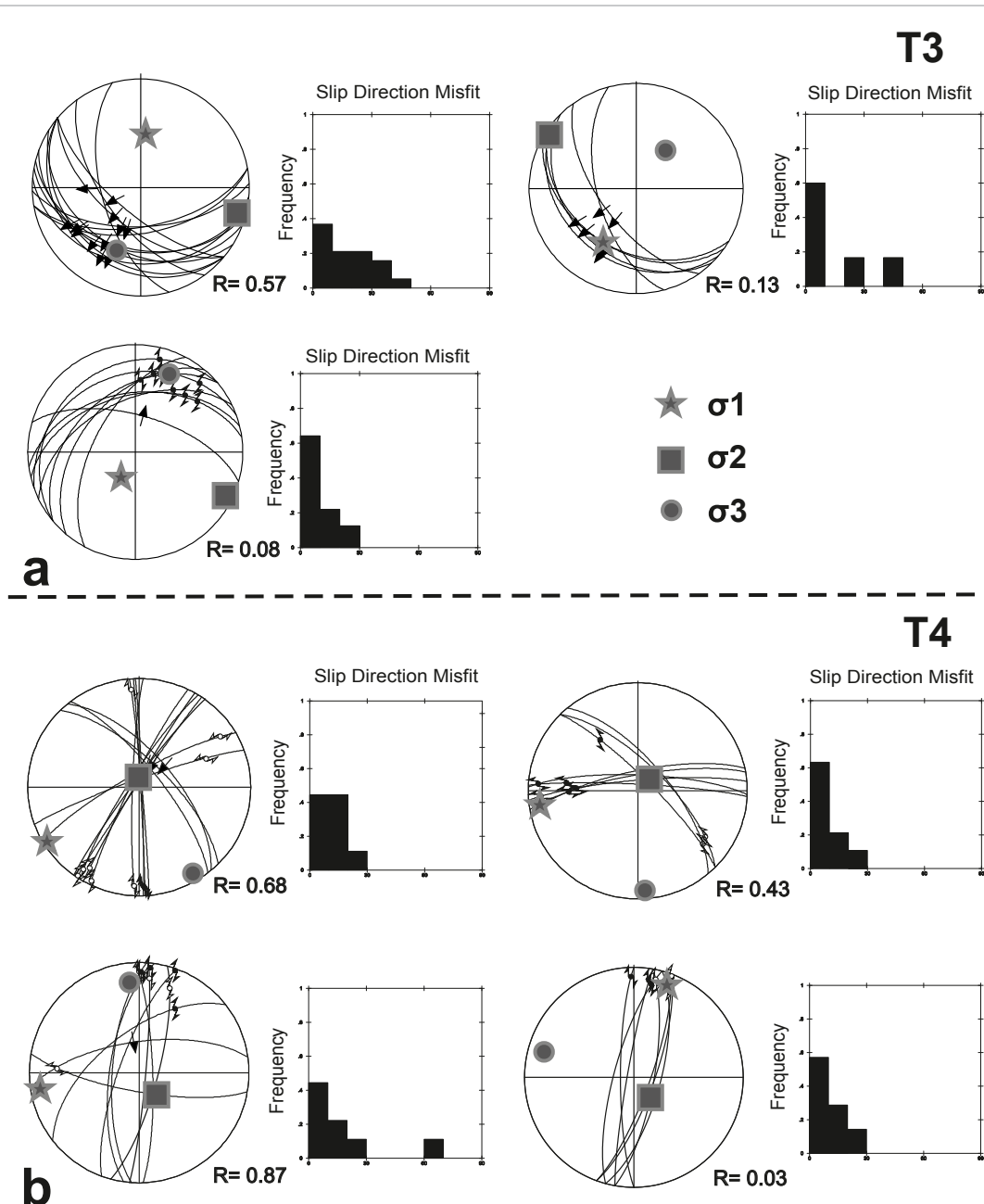
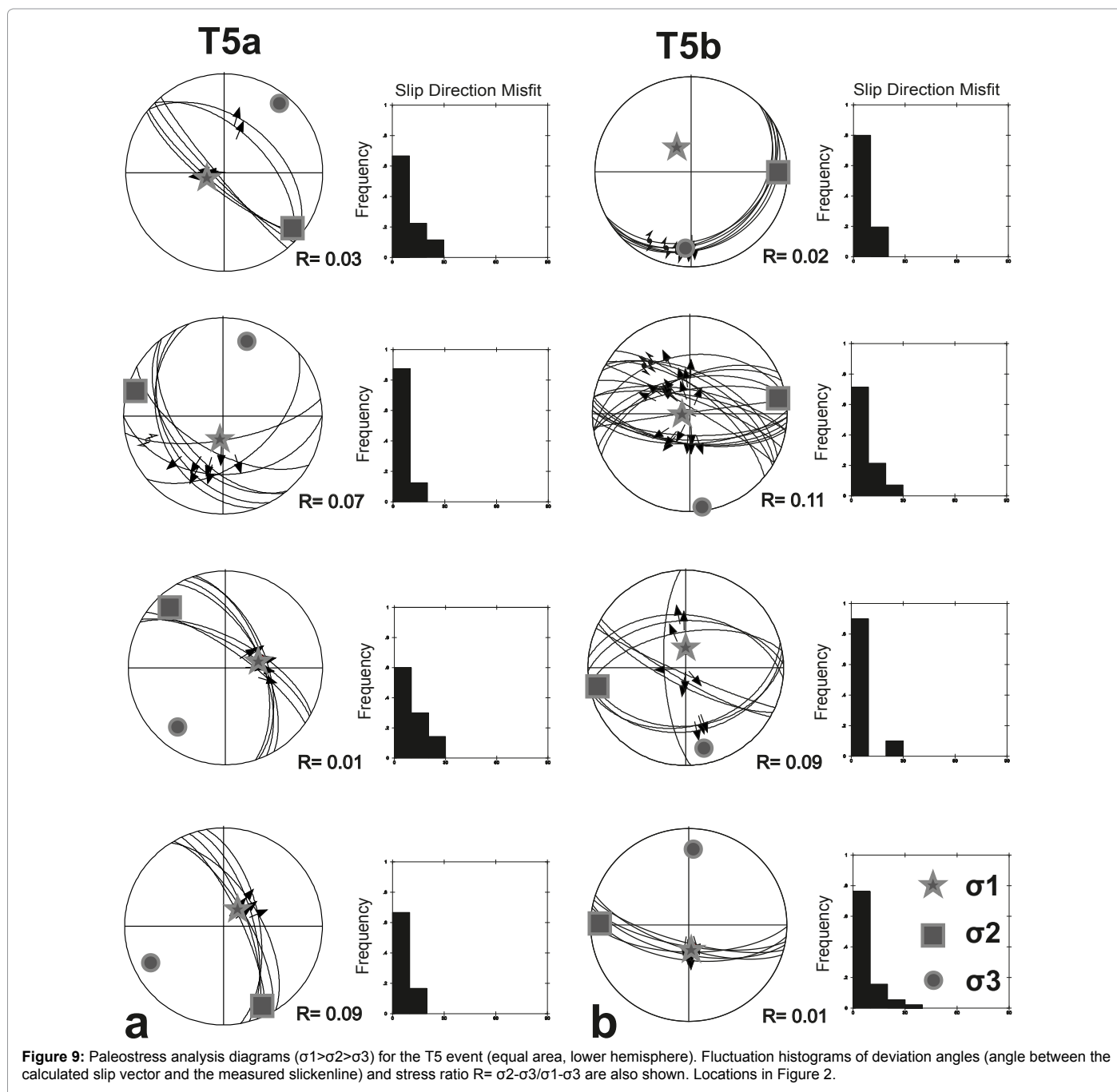


Figure 8: Paleostress analysis diagrams ($\sigma_1 > \sigma_2 > \sigma_3$) for the T3 (a) and T4 (b) events (equal area, lower hemisphere). Fluctuation histograms of deviation angles (angle between the calculated slip vector and the measured slickenline) and stress ratio $R = \sigma_2 - \sigma_3 / \sigma_1 - \sigma_3$ are also shown. Locations in Figure 2.

was characterized by a subhorizontal NE-SW oriented maximum σ_1 -stress axis and a subvertical minimum σ_3 -stress axis (Figures 4 and 8b).

Finally, extensional tectonics affected the whole area from Late Miocene to present-day related to high angle normal faults (Figures 2 and 4) (T5a), some of which are reworked as great active faults (Figures 2 and 4) (T5b). The paleostress analysis indicates the minimum σ_3 -stress axis oriented subhorizontally from NE-SW (Figure 9a) (T5a) to N-S (Figure 9b) (T5b). The last measurement develops as a relative younger orientation coinciding well with the extension direction of the recent seismic activity [28,29]. In both cases of T5a and T5b faults, the maximum σ_1 -stress axis remains almost vertical (Figure 9).

Furthermore, the conclusions of apatite fission track (AFT), as well as zircon fission tracks (ZFT) analyses, that were performed by Vamvaka et al. [12] on the detrital material in the MHT sedimentary strata and their bordering Pelagonian basement rocks (Figure 2), towards the comprehension of the MHT development, confirm the Pelagonian continent as the main source of the detrital material and meet well with the conclusions from the structural analysis. No correlation with FT ages of the western bordering basement rocks (mainly ophiolites) was available due to inappropriate lithology. Heating of the western margin of the Pelagonian continent adjacent to the MHT, during Lower-Middle Eocene, was associated to thrusting, and directly followed by fast cooling and exhumation in Middle-Upper Eocene. The



slower cooling and exhumation in the continuing during Oligocene associated to the strike-slip faults (T2) which cause localized uplift and subsidence (in the area of MHT), while less vertical movements are produced in other places (e.g., the Pelagonian continent). The Miocene extensional period (T3) is also shown from thermal modelling of track length distribution, which indicates a prolonged stay in the same temperature range (or reheating) around 25 to 10 Ma. This can be caused by crustal thinning and rise of the geothermal gradient, started already since Oligocene-Miocene time, accompanying an extensional period. In the latter thermal model, an enhanced uplift is also predicted during the last 10 Ma, which is consistent with the filling of the basin with sediments and the uplift of the area.

Geodynamically, the MHT evolved as a piggyback basin in a foreland setting above westward-emplacing ophiolites and higher Pelagonian units [6,8,11,22] while great importance is given to the role of strike-slip faults in the structural evolution of the MHT [11,12]. Successive stages and changing tectonic regimes recognised in the MHT formation are met in strike-slip basins, while experiencing alternating periods of extension and compression. The changing structural settings and repeated episodes of rapid subsidence and uplift, variable depths along the axis of the basin, asymmetry and big length-to-width ratios (4:1), axial infill subparallel to the principal displacement zones, abrupt lateral and vertical facies variations, and of course the presence of strike-slip faults, as certainly observed to bound the western side of the MHT, are some indicative features of the MHT, which constitute

typical criteria for the recognition of long-lived strike-slip zones and related basins. As the trough developed due to different tectonic events reported earlier, it corresponds to the pattern of polyhistory strike-slip basins (classification after Busby and Ingersoll) [1].

In conclusion, our interpretation for the evolution of MHT suggests successive tectonic events, in response to which MHT developed, involving isostatic crustal flexure, strike-slip faults, associated with reverse dip slip component, and normal faulting (Figure 3).

The thrace basin (THB)

Lithostratigraphy: The Thrace Basin, one of the largest Tertiary basins in the North Aegean region, is formed on the metamorphic rocks of the Rhodope massif in Northern Greece and Southern Bulgaria [14-16,30-35] as well as the Strandja and Sakarya massifs in NW Turkey, where the depocentral area of the basin is evolved (Figures 1 and 10) [36-40]. Tertiary basins (Figure 1) (Axios basin, AXB) are also referred to the Eastern Former Yugoslavian Republic of Macedonia (FYROM) by Dumurdzanov et al. [18].

Our data are focused on the part of the Thrace basin in the Greek mainland covering the Rhodope metamorphic province. Here the deposits of the THB consist of molassic-type sedimentary rocks of Paleogene age overlain unconformably by a thick (1-2 km) Neogene-

Quaternary sedimentary sequence (Figures 1 and 10) [13,17,30]. More than 90% of the total surface of the THB is covered by younger Neogene to Quaternary sediments and the Aegean Sea. About 10% of the Paleogene exposed outcrops of the basin is extended in the NE Greek mainland, from the Pangaion mountainous range until the Greek -Turkey borders, and the North Aegean islands of Limnos and Samothraki (Figures 1 and 10).

Some small outcrops of Paleogene sediments along the Axios Basin beneath Neogene-Quaternary sediments (Figure 1) [18] were regarded as equivalent infilling products to the Paleogene THB sedimentary rocks. The molassic sediments of the THB, as well as their equivalent of the Axios Basin show an age from Middle-Upper Eocene to Oligocene [13,17,41,42]. They constitute a complicated stratigraphic sequence composed by intercalation of bedded conglomerates, breccias, conglomerates, sandstones, nummulitic limestones, turbiditic layers and shales (Figure 10).

Sedimentation started during Bartonian time with initial deposition of continental sediments (mainly breccias, conglomerates and sandstones (Figure 11e), followed during the Late Eocene-Oligocene by marine turbiditic type deposits and limestones (Figure 11d). The sediments of the THB lie in places on the basement rocks of the Rhodope massif and in other places on the low-grade metamorphic

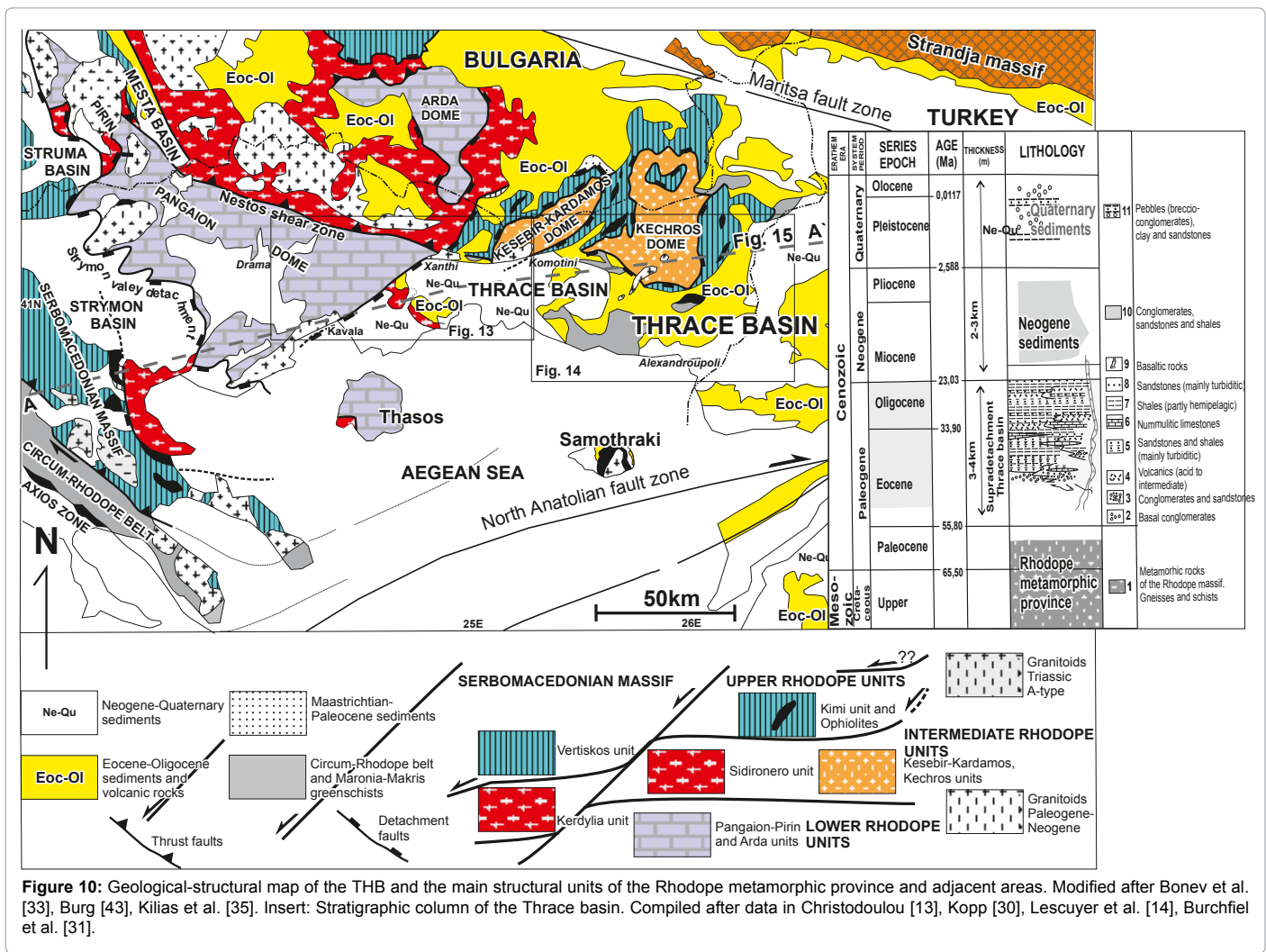


Figure 10: Geological-structural map of the THB and the main structural units of the Rhodope metamorphic province and adjacent areas. Modified after Bonev et al. [33], Burg [43], Kiliyas et al. [35]. Insert: Stratigraphic column of the Thrace basin. Compiled after data in Christodoulou [13], Kopp [30], Lescuyer et al. [14], Burchfiel et al. [31].

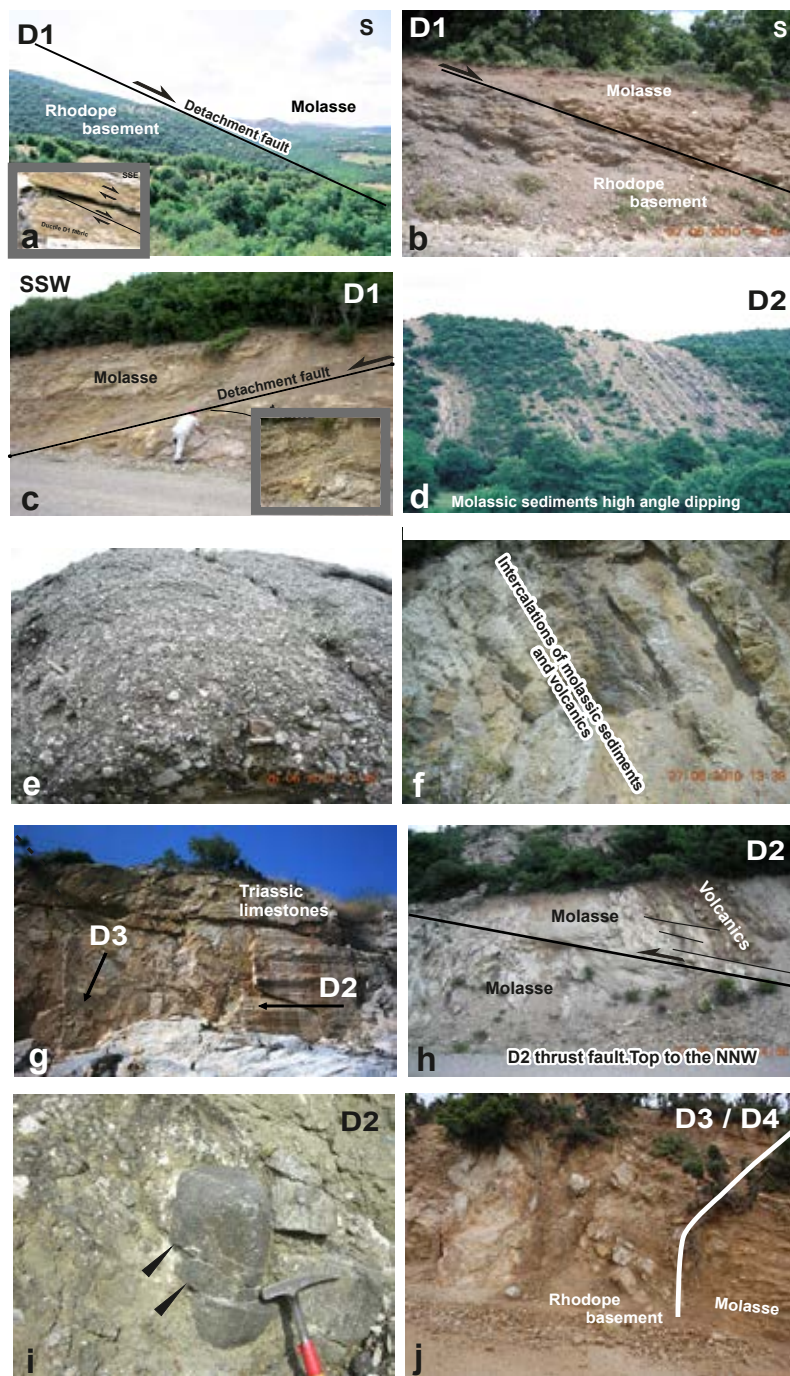


Figure 11: a, b, c. The low angle normal fault zone (D1) between the Rhodope basements rocks and THB sediments, north of Darmeni village. Shear bands in the footwall basements rocks (b, c) indicate a top to SSW sense of shear. d. High angle dipping molassic sediments (D2), at the contact near the Paterma village. e. Basal conglomerates of the THB, Paterma village. f. Intercalations of the sediments and acid to intermediate volcanic products, road Nea Santa village to Kechros village, north of the Nea Santa village. g. D2 and D3 striations on the fault plane of N-S striking fault in the Triassic marble of the Maronia-N. Makri Series, old road Komotini to Alexandroupoli cities. h. Contractional structures during the D2 kinematics in intercalations of THB sediments and volcanics, north of Darmeni village. i. Reverse faults during the D2 event, cutting pebbles components of a conglomeratic horizon in between the THB deposits, road to Drosia. j. D3 high angle fault between basement rocks and the THB sediments. On its fault plane were recognized two striation generations, the older is compatible to the D3 kinematics and the younger one to the D4. Location (2) in Figure 13.

Permo-Triassic, volcano sedimentary Maronia- Nea Makri series (Figures 10 and 11a-11c) [33,35,43]. The total thickness of the Paleogene sedimentary sequence is estimated to 2-3 km [13,30,31], although in the Turkish part of the broader Thrace Basin, where its depocenters

are developed, a thickness of about 9 km is reported [44]. Moreover, Roussos [42] refers that also in some parts of the Greek ThB, which are covered by the Neogene-Quaternary sediments or the Aegean Sea, the sedimentary deposition can reach a thickness of ca. 9 km.

The molassic-type sediments of both Thrace and Axios Basins, are intercalated by a lot of calc-alkaline and partly shoshonitic-type, acid to intermediate volcanic products of the same age, Upper Eocene to Oligocene (Figures 11f and 12-14) [18,45]. Magmatic activity was further related to gold-mineralization of great economic importance [14].

Structural evolution: Detail structural analysis and geological

mapping, as well as study of the kinematics of deformation of the sedimentary-volcanic sequence of the THB and its boundaries with the basement rocks of the Rhodope massif and Maronia-Nea Makri series, show a complicated structural evolution of the basin. It can be recorded in five progressive tectonic events (D1 to D5) from Eocene to Quaternary time (Figure 12). Subhorizontal extension dominates during the overall deformational history [35]. The direct stress inversion

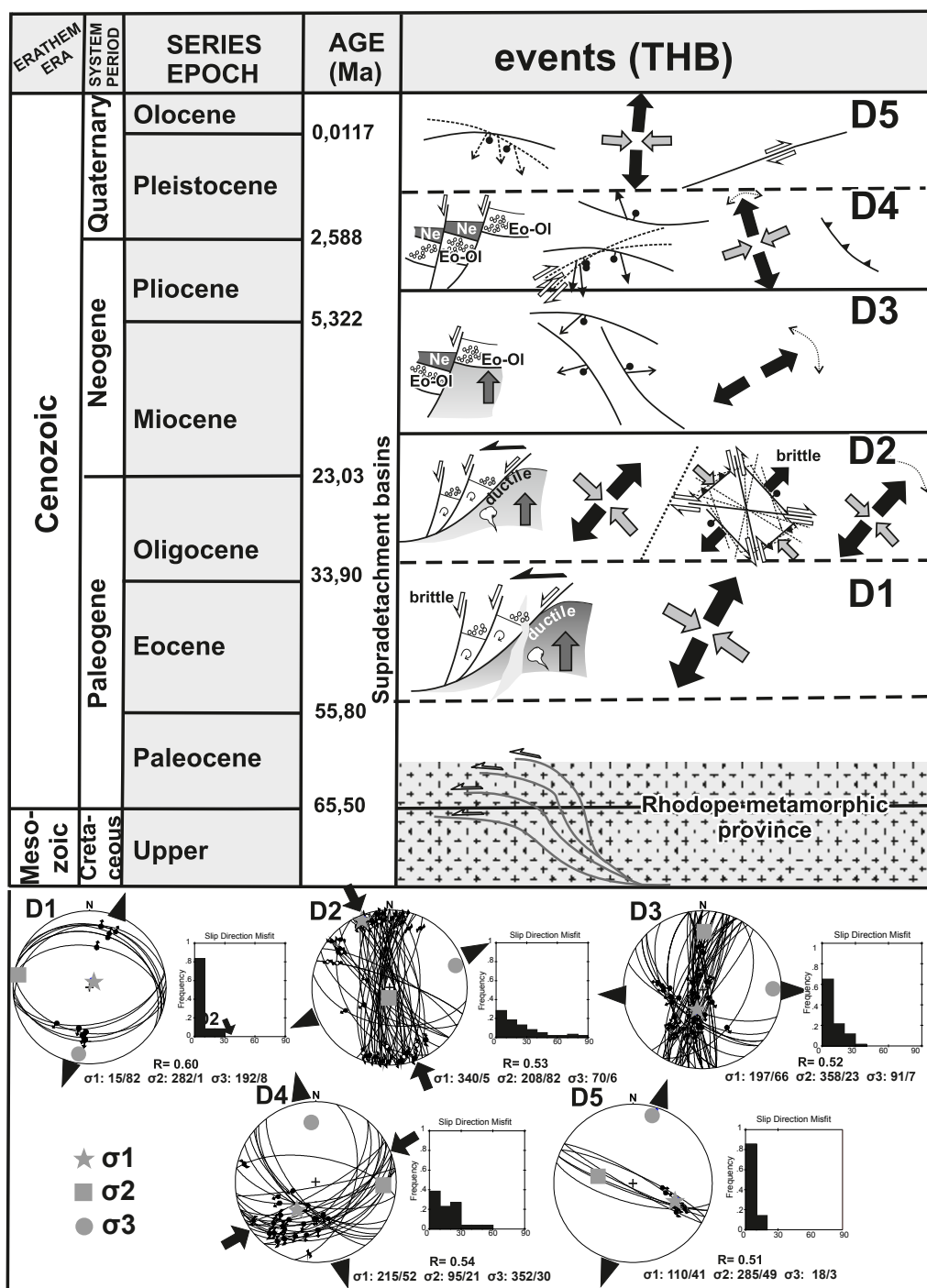


Figure 12: Distinctive features and kinematics of the main deformational events (D1 to D5) related to the THB evolutionary history. Paleostress analysis diagrams ($\sigma_1 > \sigma_2 > \sigma_3$) for each tectonic event are shown (equal area, lower hemisphere). Fluctuation histograms of deviation angles (angle between the calculated slip vector and the measured slickenline) and stress ratio $R = \sigma_2 - \sigma_3 / \sigma_1 - \sigma_3$ are also indicated (Kilias et al. 2013).

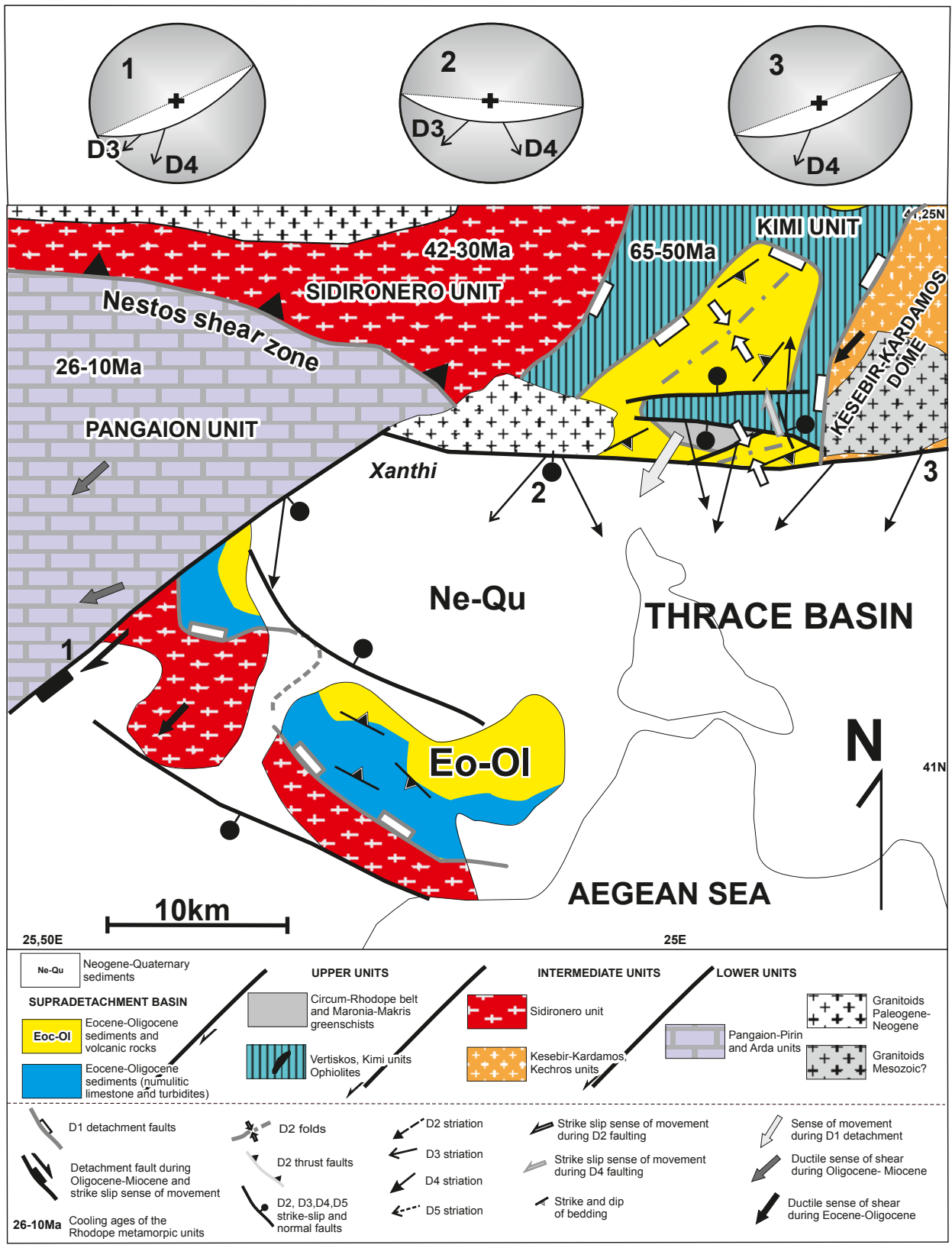


Figure 13: Detail structural map with the main fault zones and their kinematics, related to the evolutionary history of the THB (western part of the THB). The geometry of kinematics for each fault zone is shown in the stereographic diagrams (equal area, lower hemisphere). Arrows in the diagrams indicate the main development of the slickenlines on the fault planes and their relative dating (D1), according to the deformational events that have been distinguished. The numbers (1..) show the locations of the tectonic measurements.

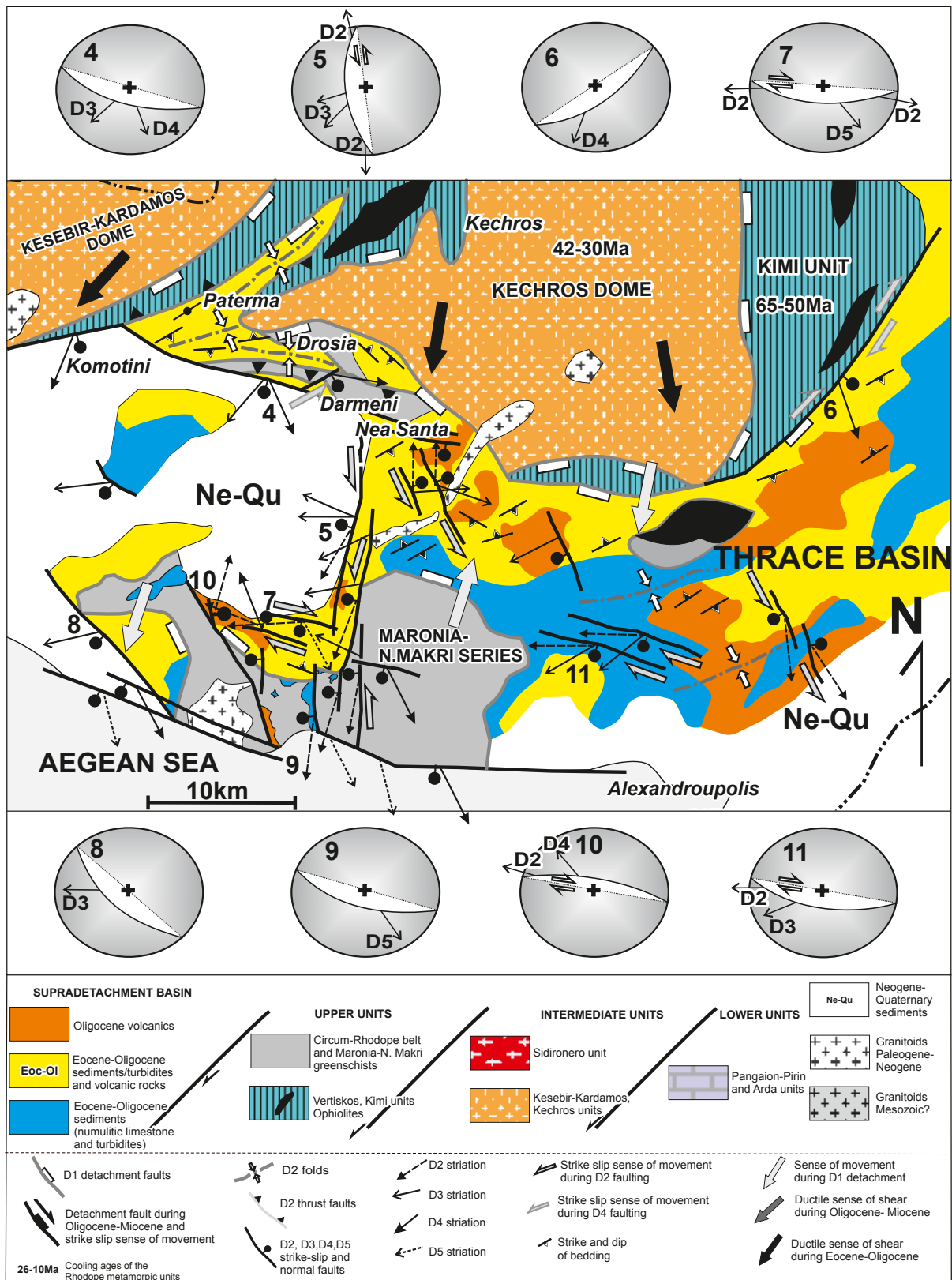


Figure 14: Detail structural map with the main fault zones and their kinematics, related to the evolutionary history of the THB (eastern part of the THB). The geometry of kinematics for each fault zone is shown in the stereographic diagrams (equal area, lower hemisphere). Arrows in the diagrams indicate the main development of the slickenlines on the fault planes and their relative dating (D1), according to the deformational events that have been distinguished. The numbers (4..) show the locations of the tectonic measurements.

method of Angelier [20,21] was also used here for the calculation of the paleostress field for each tectonic event.

D1 is characterized by low angle normal detachment faults, recognized at the tectonic boundaries of the Paleogene basin formation with the basement rocks, where no reworking took place due to younger tectonic events (Figures 11a-11c and 12-14). D1 detachment faults strike E-W to NW-SE with a main S-SW-ward dip direction. Some deviations of these rates are observed at different parts of the basin (Figures 13 and 14). Top to SW to SSW sense of shear dominates along the D1 fault planes (Figures 11a-11c) but in some places an opposite top to the NE-NNW sense of movement is also recognized related to D1 fault planes dipping to N-NE (Figures 13 and 14). The paleostress analysis indicated NE-SW to NNE-SSW trending subhorizontal minimum σ_3 - and subvertical maximum σ_1 -axes of the stress tensor (Figures 12).

D2 evolved during Oligocene-Miocene time and is related to the further reconstruction of the Thrace Basin. D2 is characterized by transpressional tectonics and formation of large conjugate strike-slip faults and extensional fractures, as well as thrust faults and folds with N-NW or S-SE sense of movement (Figures 11g-11i and 12-14). D2-extension remains again NE-SW oriented ca. parallel to the D1-extension, while compressional component of deformation is developed parallel to the Y-axis of the strain ellipsoid. During D2, the minimum principal σ_3 -stress axis is developed subhorizontal with a NE-SW to ENE-WSW trend, slightly deviated from those of the D1 event, and the maximum principal σ_1 -axis subhorizontal with a NW-SE trend, respectively (Figure 12).

D3 is responsible for high-angle normal faults dismembering the Eocene- Oligocene molassic basin into Neogene grabens (Figures 11g, 11i and 12-14). Some D2 strike-slip faults are reactivated during D3 event, as it is clearly concluded by the existence on their fault planes of oblique, to the strike-slip movements, younger D3-striations with normal sense of movement (Figure 11g). D3 event takes place during Miocene-Pliocene time while D3 extension continues about at the same orientation, NE-SW to ENE-WSW, with the earlier D1 and D2 events. The fault plane analyses yielded subvertical the maximum σ_1 -stress axis and subhorizontal ENE-WSW to E-W trending the minimum σ_3 -stress axis (Figure 12).

The D4-event is related to large WNW-ESE to NE-SW normal oblique fault zones (Figures 11j and 12-14) some of which are older, reactivated during D4, as it is indicated by the existence of at least two striations' generations on their fault planes, with the younger one to be compatible with the D4 kinematics (Figures 13 and 14). D4 structures are of Pliocene-Pleistocene age, characterized also by minor oblique reverse faults. Extension orientation changes slightly during D4 to NNW-SSE, associated with a subhorizontal ENE-WSW contraction. Stress tensor during D4 was calculated with the minimum σ_3 -axis at a NNW-SSE to NNE-SSW bearing and the maximum σ_1 - axis at an ENE-WSW to ESE-WNW direction, both with a low to moderate plunge, respectively (Figure 12).

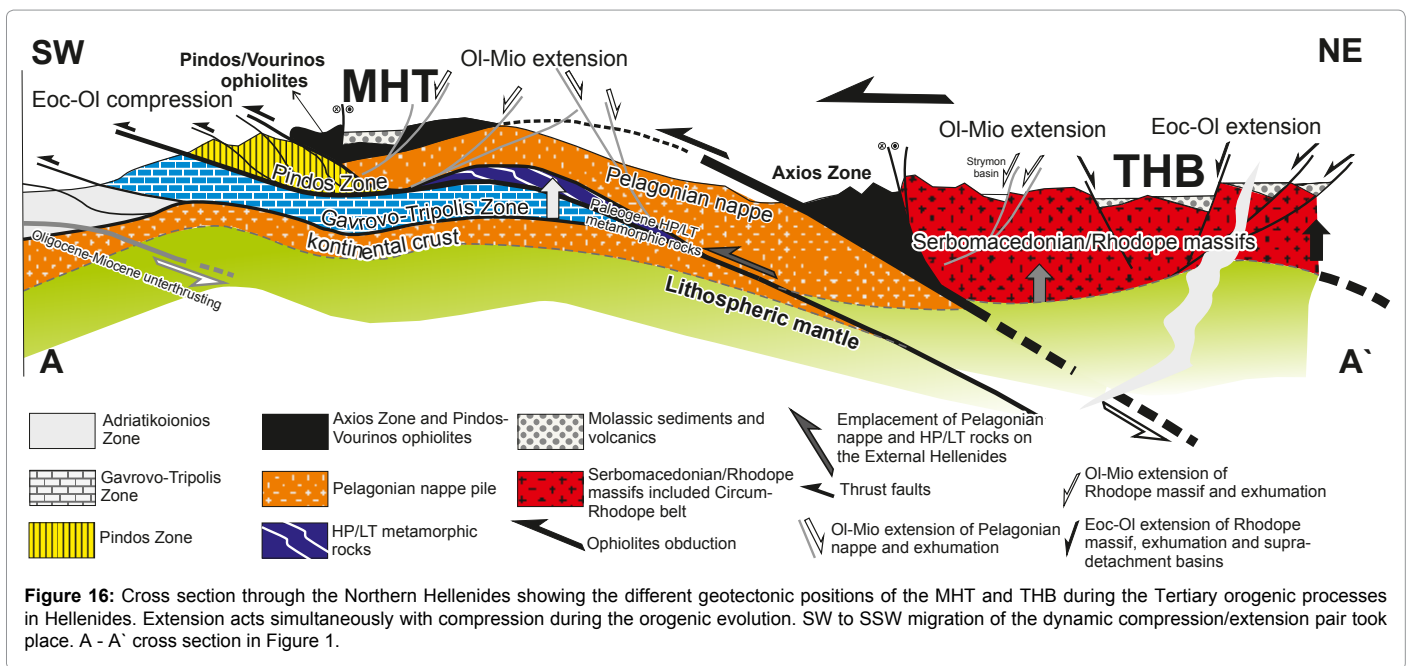
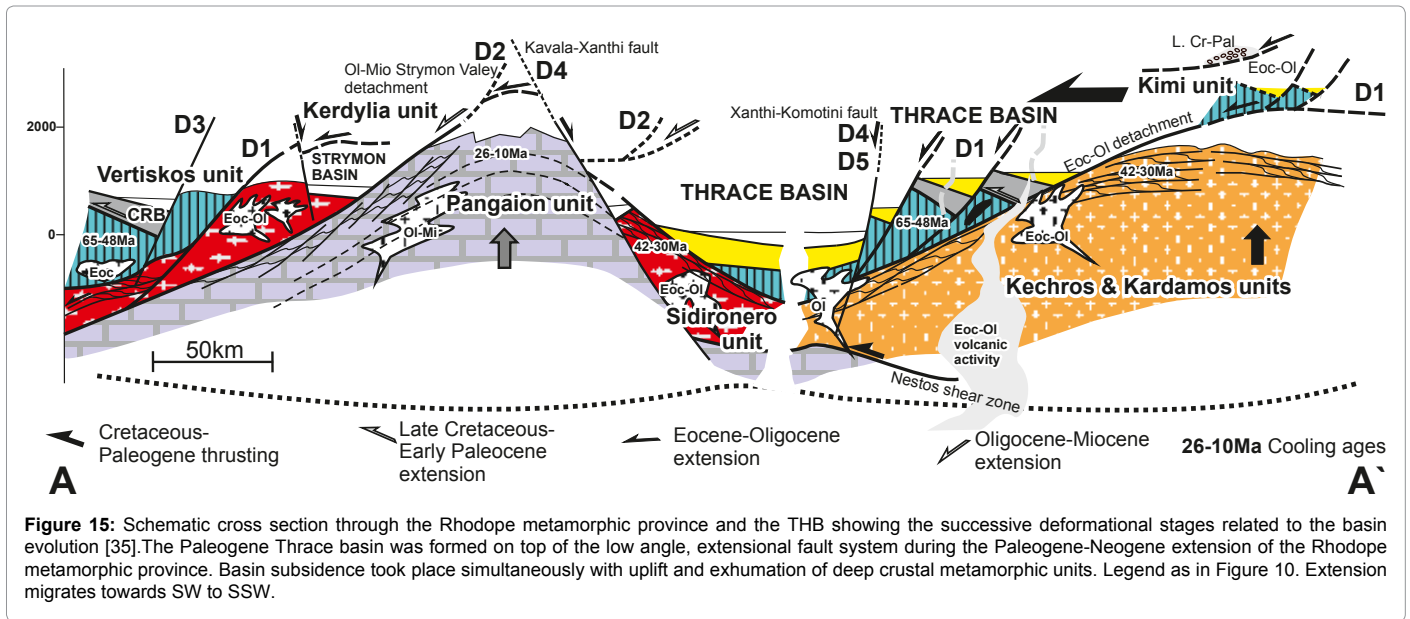
Some of the D4 fault zones remain active until present time (D5). They form large active faults reactivated during the present stress field in the area defined by the earthquake focal mechanisms and characterized by a NNE- SSW oriented subhorizontal extension (Figures 12-14). The paleostress analysis of the D5 active faults revealed a minimum σ_3 -stress axis subhorizontal with NNE-SSW bearing (i.e. 10 ° to 30 °) (Figure 12) which coincides exactly with the active extension in the broader area, as it is concluded from the local mechanisms of the strong earthquakes [28].

We interpret the Paleogene part of the THB in the NE Greek mainland as a supradetachment basin [35], as it is shown by the syntectonic deposition of the Paleogene molassic strata of the THB on the fault planes of the extensional detachment faults, related to the stretching and progressive exhumation of the Rhodope metamorphic nappe pile during the Tertiary (Figure 15) [33,35,43,46-49]. The Paleogene volcano sedimentary infilling of the Axios Basin is regarded as equivalent to the Greek Thrace Basin sedimentary sequence.

Geotectonic setting-discussion

Molassic-type sedimentation starts in both basins, MHT and THB including the Paleogene sequence of the Axios Basin, simultaneously during Mid-Late Eocene time (Bartonian-Priabonian), but it finishes at different time, at the Mid-Late Miocene for the MHT and the Late Oligocene for the THB and its equivalent part of the Axios Basin. This Tertiary, westwards progressive delay of the sedimentary stoppage in both areas, is compatible with the W-SW-wards orogen migration of the Hellenides during the Tertiary [49]. Neogene-Quaternary sediments lie discordantly on the molassic deposits of the basins, forming the last intramontane basins of Hellenides. Furthermore, the THB and its equivalent sequence of the Axios Basin is characterized by abundant volcanic products associated with granitoid intrusions of similar age into the Rhodope basement rocks under syn- to late orogenic extension [32,50]. Nevertheless, important strike-slip movements of Oligocene-Miocene age associated with transpressional or transtensional structures are common during both basins' evolution, showing the great significance of such strike-slip movements along the Hellenides during the Tertiary. Both basins show further analogous deformational setting during the Neogene-Quaternary time with the development of local compressional structures followed again by a general extension regime. Active faults with about the same kinematics, NNE- SSW for the THB and NNW-SSE for the MHT, dominate also in both areas.

The MHT was evolved as an intramontane piggy-back basin above the ophiolitic nappe and the higher Pelagonian units, during their westward traveling upon the cold Hellenic accretionary prism (Figures 3 and 16). This geotectonic position, on the cold accretionary prism (Lower plate), interprets well the total lack of any magmatic activity during the basin evolution. Initial isostatic crustal flexure associated possibly with back-thrusting toward east (Mid-Upper Eocene), strike-slip faulting (Oligocene-Miocene) and finally normal detachment faulting towards west (Lower-Middle Miocene) were the main motor mechanisms related to the basin evolution [11,12]. This differs from previous interpretations, from Doutsos et al. [6] that envisaged foreland depression related to continue, from Eocene to Miocene, back thrusting towards east or from Ferriere et al. [8] who suggest that the MHT originated as a forearc basin during the first stages of a Mid-Late Eocene subduction (Pindos basin) and evolved into a piggy-back basin as a result of Oligocene underthrusting of the large thick-crust Gavrovo-Tripolis domain. In contrast to the MHT, at least the studied part of the Greek THB, including the Paleogene deposits of the Axios Basin, evolved as a Paleogene supra detachment basin above the strongly stretched, during the Eocene-Oligocene, Internal Hellenides (Figures 15 and 16) [33,49]. Exhumation of deep crustal levels took place about simultaneously with basin subsidence and migration of deformation towards W-SW, as well as with the progressive change of the tectonic conditions from ductile to brittle during the Paleogene - Neogene [35,49]. The origin of the Upper Eocene-Oligocene syndepositional magmatic activity could be attributed to the subduction processes evolved during the Paleogene more further to the W-SW in Pindos



or Axios ocean(s). So that it is concluded that extension and basin formation in the Rhodope province took place simultaneously with contraction, nappe stacking and crustal thickening as well as HP/LT metamorphism at the more external parts of the Hellenides towards the foreland (Figure 16) [25,26,51-53].

However, Marchev et al. [32] explain the origin of the Paleogene magmatism and the simultaneous extension and crustal thinning of the Rhodope continental crust due to convective removal of the lithosphere and mantle diapirism, while Maravelis et al. and Tranos [16,34] regard the Thracian Basin as a fore-arc basin but without clear evidence about the existence or position of a Tertiary accretionary prism associated to the basin formation. Furthermore, their main investigations were focused in the Limnos island at the southernmost continuation of the THB.

Conclusions

In conclusion, according to our descriptions about the structural evolution and stratigraphic features of the MHT and THB (including the Axios Basin), we assume that both basins constitute independent basin structures, evolved in different geotectonic positions and do not represent lateral continuation. The THB evolved on the stretched and thinned upper plate of the Hellenic hinterland, above of a subducted slab of the lower plate during the Tertiary (Figure 16). Basin subsidence was associated with tectonic denudation and exhumation of deep crustal metamorphic rocks of the Rhodope province, as well as with abundant magmatic products. The MHT was evolved on the cold, thick crustal part of the External Hellenides, in the foreland area behind the Tertiary accretionary prism of the Hellenides and the Tertiary subduction zone (lower plate during the Tertiary orogenic processes),

so that no important magmatic activity accompanied the sediments deposition during the basin evolution (Figure 16).

In any case, the tectonic history of both basins seems to be related to an overall oblique plate convergence of the Apulia plate and the Internal Hellenides units during the Tertiary, as it could be inferred by the important Tertiary strike-slip motions dominated in both areas [11,12,54,55].

Acknowledgments

The research was supported by the projects "Pythagoras II" by GSRT and the "Excellence Post-doc Scholarship" by RC AUTH.

References

- Busby CJ, Ingersoll RV (1995) *Tectonics of sedimentary basins*. Blackwell Science Cambridge Oxford Mass USA, 579 pp.
- Einsele G (2000) *Sedimentary basins*. 2 Auflage Springer Verlag, Berlin 792 pp.
- Friedmann SJ, Burbank DW (1995) Rift basins and supradetachment basins: Intracontinental extensional end-members. *Basin Research* 7: 109-127.
- McCloughry JD, Gaylord DR (2005) Middle Eocene sedimentary and volcanic infilling of an evolving supradetachment basin: White Lake Basin, south-central British Columbia. *Can J of Earth Sci* 42: 49-66.
- Brunn JH (1956) Contribution the geological study of Northern Pindos and part of Western Macedonia. *Ann Geol Pays Hellenique* 7: 1-346.
- Doutsos T, Koukouvelas I, Zeliidis A, Kontopoulos N (1994) Intracontinental wedging and post-orogenic collapse in the Mesohellenic trough. *Geolog Rundschau* 83: 257-275.
- Zeliidis A, Piper DJW, Kontopoulos N (2002) Sedimentation and basin evolution of the Oligocene-Miocene Mesohellenic basin, Greece. *AAPG* 86: 161-182.
- Ferriere J, Reynaud JY, Pavlopoulos A, Bonneau M, Migros G (2004) Geologic evolution and geodynamic controls of the Tertiary intramontane piggyback Meso- Hellenic Basin, Greece. *Bull Soc Geol France* 175: 361-381.
- Ferriere J, Chanier F, Reynaud JY, Pavlopoulos A, Ditbanjong P (2011) Tectonic control of the Meteora conglomerates (Meso-Hellenic Basin, Greece). *Bull Soc Geol France* 182: 437-450.
- Ferriere J, Chanier F, Reynaud J, Pavlopoulos A, Ditbanjong P (2013) Evolution of the Mesohellenic Basin (Greece): a synthesis. In: Skourtsos E (ed), *the Geology of Greece - Part II*. Journal of the Virtual Explorer Electronic Edition 452 pp.
- Vamvaka A, Kilias A, Mountrakis D, Papoikononou J (2006) Geometry and structural evolution of the Mesohellenic Trough (Greece), a new approach. *Geological Society of London, Special Publications* 260: 521-538.
- Vamvaka A, Spiegel C, Frisch W, Danisik M, Kilias A (2010) Fission track data from the Mesohellenic Trough and the Pelagonian zone in NW Greece: Cenozoic tectonics and exhumation of source areas. *Intern Geol Review* 52: 223-248.
- Christodoulou G (1958) About the age of some formations of Samothrace. *Bull Geol Soc Greece* 3: 40-45.
- Lescuyer JL, Bailly L, Cassard D, Lips ALW, Piantone P et al. (2003) Sediment hosted gold in south-eastern Europe: the epithermal deposit of Perama, Thrace, Greece. In: Eliopoulos DG (ed), *Mineral exploration and sustainable development*. Millpress Rotterdam 499-502 pp.
- Kilias A, Falalakis G, Gemitzi A, Christaras V (2006) Faulting and paleostress evolution in the Maronia-Petrota basin. Evidence of active faults. *Bull Tethys Geol Soc* 1: 7-16.
- Maravelis A, Konstantopoulos P, Pantopoulos G, Zeliidis A (2007) North Aegean sedimentary basin evolution during the Late Eocene to Early Oligocene based on sedimentological studies on Lemnos island (NE Greece). *Geol Carpathica* 58: 455-464.
- Mainhold G, BonDagher-Fadel M (2010) Geochemistry and biostratigraphy of Eocene sediments from Samothraki island, NE Greece. *N Jb Geol Palaeont Abh* 256: 17-38.
- Dumurdzanov N, Serafimovski T, Burchfiel BC (2005) Cenozoic tectonics of Macedonia and its relation to the South Balkan extensional regime. *Geosphere* 1: 1-22.
- Kontopoulos N, Fokianou T, Zeliidis A, Alexiadis C, Rigakis N (1999) Hydrocarbon potential of the middle Eocene-middle Miocene Mesohellenic piggyback basin (central Greece): a case study. *Mar and Petrol Geol* 16: 811-824.
- Angelier J (1979) Determination of the mean principal direction of stresses for a given fault population. *Tectonophysics* 56: T17-T26.
- Angelier J (1990) Inversion of field data in fault tectonics to obtain the regional stress-field: A new rapid direct inversion method by analytical means. *Geoph J Intern* 103: 363-376.
- Wilson J (1993) The anatomy of Krania basin, northwest Greece. *Bull Soc Geol Greece* 28: 361-368.
- Zygogiannis N, Muller C (1982) Nannoplankton biostratigraphy der tertiären Mesohellenischen molasses (Northwest Greece). *Z dtgeol Gesel* 133: 445-455.
- Pangaea Software Scientific, MyFault, version 1.03.
- Kilias A, Fasoulas C, Priniotakis M, Sfeikos A, Frisch W (1991) a. Deformation and HP-LT metamorphic conditions at the tectonic window of Kranea (W Thessaly, Northern Greece). *Z dtgeol Ges* 142: 87-96.
- Kilias A, Frisch W, Ratschbacher L, Sfeikos A (1991) b. Structural evolution and metamorphism of blueschists, Ampelakia nappe, eastern Thessaly, Greece. *Bull Geol Soc Greece* 25: 81-89.
- Sfeikos A, Boehringer C, Frisch W, Kilias A, Ratschbacher L (1991) Kinematics of Pelagonian nappes in Kranea area, North Thessaly. *Bull Geol Soc Greece* 25: 101-105.
- Papazachos BC, Papadimitriou EE, Kiratzi AA, Papazachos CB, Louvari EK (1998) Fault plane solutions in the Aegean Sea and the surrounding area and their tectonic implications. *Boll di Geof Teorica ed Applicata* 39: 199-218.
- Mountrakis D, Pavlides S, Zouros N, Astaras Th, Chatzipetros A (1998) Seismic fault geometry and kinematics of the 13 May 1995 western Macedonia (Greece) earthquake. *Journal of Geodynamics* 26: 175-196.
- Kopp KO (1965) *Geologie Thrakiens III: Das Tertiaer zwischen Rhodope und Evros*, *Ann. Geol Pays Hellenique* 16: 315-362.
- Burchfiel BC, Nakov R, Tzankov T (2003) Evidence from the Mesta half-graben, SW Bulgaria, for the Late Eocene beginning of Aegean extension in the Central Balkan Peninsula. *Tectonophysics* 375: 61-76.
- Marchev P, Kaiser-Rohrmeier M, Heinrich C, Ovtcharova M, von Quadt A et al. (2005) Hydrothermal ore deposits related to post-orogenic extensional magmatism and core complex formation: The Rhodope Massif of Bulgaria-Greece. *Ore Geol Rev* 27: 53-89.
- Bonev N, Burg JP, Ivanov Z (2006) Mesozoic-Tertiary structural evolution of an extensional gneiss dome - The Kesebir-Kardamos dome, eastern Rhodope (Bulgaria-Greece). *Intern J Earth Sci* 95: 318-340.
- Tranos M (2009) Faulting of Lemnos island: a mirror of the North Aegean Trough (Northern Greece). *Tectonophysics* 467: 72-88.
- Kilias A, Falalakis G, Sfeikos A, Papadimitriou E, Vamvaka A et al. (2013) The Thrace basin in the Rhodope province of NE Greece - A tertiary supradetachment basin and its geodynamic implications. *Tectonophysics* 595: 90-105.
- Turgut T, Tuerkaslan M, Perincek D (1991) Evolution of the Thrace sedimentary basin and its hydrocarbon prospectivity. In: Spencer AM (ed) *Generation, Accumulation and Production of Europe's Hydrocarbon*. Special Public European Association Petroleum Geosciences, 415-437 pp.
- Turgut S, Eseller G (2000) Sequence stratigraphy, tectonics and depositional history in eastern Thrace Basin, NW Turkey. *Mar and Petr Geol* 17: 61-100.
- Siyako M, Huvaz O (2007) Eocene stratigraphic evolution of the Thrace Basin, Turkey. *Sedim Geol* 198: 75-91
- Okay A, Oezcan E, Cavazza W, Okay N, Less G (2010) Upper Eocene olistostromes, two contrasting basement types and the initiation of the Thrace basin, NW Turkey. *Turkish J of Earth Sci* 19: 1-24.
- Cavazza W, Federici I, Okay A, Zattin M (2012) Apatite fission-track thermochronology of the Western Pontides (NW Turkey). *Geol Mag* 149: 133-140.

41. Dragomanov LK, Grigorov V, Ioncher A, Jeleu A, Darakchieva St (1986) Lithological indications of the presence of Middle Eocene in the Eastern Rhodopes. *Ann. Higher Inst Mining Geol* 32: 37-41.
42. Roussos N (1994) Stratigraphic and paleogeographic evolution of the Paleogene Molassic basins of the Northern Aegean. *Bull Geol Soc Greece* 32: 275-294.
43. Burg JP (2012) Rhodope: From Mesozoic convergence to Cenozoic extension. Review of petro-structural data in the geochronological frame. *The Geology of Greece Journal of virtual Explorer* 42: 1-44.
44. Goeruer N, Okay AJ (1996) Afore-arc origin for the Thrace basin, NW Turkey. *Geol Rundsch* 85: 662-668.
45. Christofides G, Pecskey Z, Eleftheriadis G, Soldatos T, Koroneos A (2004) The Tertiary Evros volcanic rocks (Thrace, Northeastern Greece): Petrology and K/Ar geochronology. *Geol Carpathica* 55: 397-409.
46. Dinter DA, Royden L (1993) Late Cenozoic extension in northeastern Greece: Strymon Valley detachment system and Rhodope metamorphic core complex. *Geology* 21: 45-48.
47. Dinter DA, Macfarlane AM, Hames W, Isachsen C, Bowring S, et al. (1995) U-Pb and ⁴⁰Ar/³⁹Ar geochronology of Symvolon granodiorite: implications for the thermal and structural evolution of the Rhodope metamorphic core complex, Northeastern Greece. *Tectonics* 14: 886-908.
48. Brun JP, Sokoutis D (2007) Kinematics of the Southern Rhodope Core Complex (North Greece). *Intern J Earth Sci* 99: 109-138.
49. Kilias A, Falalakis G, Mountrakis D (1999) Cretaceous-Tertiary structures and kinematics of the Serbomacedonian metamorphic rocks and their relation to the exhumation of the Hellenic hinterland (Macedonia, Greece). *Intern J Earth Sci* 88: 513-531.
50. Kilias A, Mountrakis D (1998) Tertiary extension of the Rhodope massif associated with granite emplacement (Northern Greece). *Acta Vulcanologica* 10: 331-337.
51. Schermer RE, Lux DR, Burchfiel BC (1990) Temperature-Time history of subducted continental crust, Mt. Olympos region, Greece. *Tectonics* 9: 1165-1195.
52. Schermer ER (1993) Geometry and kinematics of continental basement deformation during the Alpine orogeny, Mt. Olympos region, Greece. *J Struct Geol* 15: 571-591.
53. Ring U, Glodny J, Thomson S (2010) The Hellenic subduction system: high-pressure metamorphism, exhumation, normal faulting and large scale extension. *Ann Rev of Earth and Plan Sci* 38: 45-76.
54. Tranos MD, Kilias A, Mountrakis D (1999) Geometry and kinematics of the Tertiary post-metamorphic Circum Rhodope Belt Thrust System (CRBTS), Northern Greece. *Bull Soc Geol Greece* 33: 5-16.
55. Papanikolaou D, Lekkas E, Mariolakos E, Mirkou R (1988) Contribution on the geodynamic evolution of the Mesohellenic trough. *Bull Geol Soc Greece* 20: 17-36.